Molecular Biology of the Cell
Vol. 20, 2744–2754, June 1, 2009

Autophagic Elimination of Misfolded Procollagen Aggregates in the Endoplasmic Reticulum as a Means of Cell Protection

Yoshihito Ishida,* Akitsugu Yamamoto,† Akira Kitamura,*‡ Shireen R. Lamandé,§ Tamotsu Yoshimori,‖ John F. Bateman,§ Hiroshi Kubota,*¶ and Kazuhiro Nagata*

*Department of Molecular and Cellular Biology, Institute for Frontier Medical Sciences, Kyoto University, Sakyo-ku, Kyoto 606-8397, Japan; †Department of Cell Biology, Nagahama Institute of Bio-Science and Technology, Nagahama, Shiga 526-0829, Japan; §Murdoch Children's Research Institute, Royal Children's Hospital, Parkville, Victoria 3052, Australia; and ‖Department of Cell Regulation, Research Institute for Microbial Diseases, Osaka University, Suita-Osaka 565-0871, Japan

Submitted November 3, 2008; Revised March 26, 2009; Accepted April 1, 2009
Monitoring Editor: Jeffrey L. Brodsky

Type I collagen is a major component of the extracellular matrix, and mutations in the collagen gene cause several matrix-associated diseases. These mutant procollagens are misfolded and often aggregated in the endoplasmic reticulum (ER). Although the misfolded procollagens are potentially toxic to the cell, little is known about how they are eliminated from the ER. Here, we show that procollagen that can initially trimerize but then aggregates in the ER are eliminated by an autophagy-lysosome pathway, but not by the ER-associated degradation (ERAD) pathway. Inhibition of autophagy by specific inhibitors or RNAi-mediated knockdown of an autophagy-related gene significantly stimulated accumulation of aggregated procollagen trimers in the ER, and activation of autophagy with rapamycin resulted in reduced amount of aggregates. In contrast, a mutant procollagen which has a compromised ability to form trimers was degraded by ERAD. Moreover, we found that autophagy plays an essential role in protecting cells against the toxicity of the ERAD-inefficient procollagen aggregates. The autophagic elimination of aggregated procollagen occurs independently of the ERAD system. These results indicate that autophagy is a final cell protection strategy deployed against ER-accumulated cytotoxic aggregates that are not able to be removed by ERAD.

INTRODUCTION

The biosynthesis of secretary and membrane proteins in the endoplasmic reticulum (ER) is strictly monitored by a mechanism called ER quality control to ensure that only properly folded and assembled proteins are allowed to reach their final destination (Anelli and Sitia, 2008). Misfolded or aberrant proteins produced by mutations or various stresses are retrotranslocated from the ER into the cytosol for degradation by the 26S proteasome after modification with polyubiquitin chains, by a process called ER-associated degradation (ERAD) (Ron and Walter, 2007). During the ERAD process, misfolded proteins are recognized by the ER-degradation enhancing α-mannosidase-like protein (EDEM) that presumably targets the protein for retrotranslocation and degradation (Oda *et al.,* 2003). Very recently, we have shown that a supramolecular complex containing the ER-resident disulfide-reductase ERdj5, which is the molecular chaperone BiP, and EDEM mediates ERAD of glycoproteins (Ushioda *et al.,* 2008). ERAD substrates are transferred from the ER to the cytosol as unfolded polypeptide chains through translocon channel. However, how other toxic species, such as severely aggregated proteins, are eliminated from the ER is largely unknown.

In addition to ERAD, autophagy-mediated lysosomal degradation of ER proteins has also been reported (Vembar and Brodsky, 2008). Autophagy (macroautophagy) is a catabolic process that degrades cellular organelles, exogenous viruses, and bacteria in the cytoplasm (Klionsky, 2007; Mizushima *et al.,* 2008). Autophagy mainly consists of three steps: formation of an autophagosome with a double membrane, sequestration of cytoplasmic constituents, and fusion of the autophagosome with lysosomes, where encapsulated constituents are degraded by proteases. A large number of factors essential for autophagosome formation have been identified in yeast and mammals (Klionsky, 2007; Suzuki and Ohsumi, 2007). Analyses of *Atg5*-null, *Atg7*-null or *Atg7* conditional knockout mice have revealed that autophagy is indispensable for the constitutive clearance of misfolded toxic proteins in the cytosol, particularly in the CNS, liver, and heart (Komatsu *et al.,* 2007a,b).

This article was published online ahead of print in *MBC in Press* (http://www.molbiolcell.org/cgi/doi/10.1091/mbc.E08–11–1092) on April 8, 2009.

Present addresses: ‡Laboratory of Molecular Cell Dynamics, Faculty of Advanced Life Science, Hokkaido University, Kita 21 Nishi 11, Kita-ku, Sapporo 001-0021, Japan; ¶Department of Life Science, Faculty of Engineering and Resource Science, Akita University, 1-1 Tegata-Gakuencho, Akita 010-8502, Japan.

Address correspondence to: Kazuhiro Nagata (nagata@frontier.kyoto-u.ac.jp).

Abbreviations used: ATZ; α1-antitrypsin Z variant; EDEM, ER-degradation enhancing α-mannosidase-like protein; ER, endoplasmic reticulum; ERAD, endoplasmic reticulum–associated degradation; Hsp47, 47-kDa heat-shock protein; NHK, α1-antitrypsin Null Hong Kong variant; OI, osteogenesis imperfecta.

© 2009 by The American Society for Cell Biology

Recently, Kruse *et al.* (2006) reported using yeast ATG6-deletion mutant that an α1-antitrypsin Z variant (ATZ) that accumulated in the ER was degraded via autophagy as well as ERAD, and a similar autophagy-dependent degradation of ATZ was reported in ATG5 knockout mammalian cells (Kamimoto *et al.*, 2006). More recently, a dysferlin mutant, which causes limb girdle muscular dystrophy type 2B, has been reported to be degraded via autophagy and ERAD (Fujita *et al.*, 2007). However, the molecular mechanism of autophagy-dependent clearance of misfolded and/or aggregated proteins that accumulate in the ER is largely unknown, and little is known about what effect autophagic clearance of toxic aggregates that accumulate in the ER has on cell survival.

Collagen is a major component of the extracellular matrix essential for supporting and organizing most tissues. Type I collagen molecule is a trimer of two proα1(I) chains and one proα2(I) chain, and triple helix formation of the collagen occurs in the ER. Mutations in the *COL1A1* or *COL1A2* genes, including insertions, deletions, and point mutations in the helical domains (Gajko-Galicka, 2002; Marini *et al.*, 2007), disrupt proper formation of the triple helix and cause severe bone fragility including osteogenesis imperfecta (OI) (Rauch and Glorieux, 2004). Folding of procollagen requires the collagen-specific molecular chaperone Hsp47 in the ER, in addition to general ER chaperones including calnexin, BiP, Grp94, and protein disulfide isomerase (PDI; Lamande and Bateman, 1999; Nagata, 2003). Disruption of the *hsp47* gene causes embryonic lethality by 11.5 days after coitus due to defects in the formation of collagen fibrils and basement membranes (Nagai *et al.*, 2000; Marutani *et al.*, 2004; Matsuoka *et al.*, 2004). In vitro analysis using *hsp47*-disrupted fibroblasts revealed that triple helix formation, secretion, and processing of the N-terminal propeptide of type I collagen are impaired (Matsuoka *et al.*, 2004; Ishida *et al.*, 2006). We also reported that misfolded type I collagen in Hsp47-null cells formed detergent insoluble aggregates in the ER (Ishida *et al.*, 2006). However, little is known about how these potentially toxic aggregates are eliminated from the ER.

Here, we have explored the fate of misfolded and insoluble procollagens that have accumulated in the ER, caused either by the disruption of the collagen-specific molecular chaperone Hsp47 or by the OI-causing mutation disrupting the triple-helical domain of the proα1(I) chain. We show that misfolded procollagens accumulated as aggregates in the ER cannot be removed by the ERAD, but are eliminated through autophagy. Intriguingly, inhibition of autophagy by RNAi-mediated knockdown resulted in increased cell death concomitant with enhanced accumulation of aggregated collagen in the ER. These observations demonstrate that autophagy exerts an essential role in cell survival against the cytotoxicity of ERAD-inefficient misfolded proteins. Furthermore, we also demonstrate that under the conditions where misfolded and detergent-insoluble procollagens are accumulated in the ER, the ERAD pathway is still available for the degradation of other misfolded proteins. Thus, for the elimination of ER-accumulated aggregates, the autophagy system appears to be independent of the ERAD system. We discuss the biological significance of autophagic clearance of misfolded proteins from the ER as an alternative protective strategy in cell survival.

MATERIALS AND METHODS

Expression Vectors

Expression vectors of proα1(I) chain (Stephens and Pepperkok, 2002), green fluorescent protein (GFP)-LC3 (Kabeya *et al.*, 2000), α1-antitrypsin Null Hong Kong (NHK) variant (Hosokawa *et al.*, 2006), and an inactive mutant of ATG4B fused with mStrawberry, which is a variant of red fluorescence prtotein (RFP; Fujita *et al.*, 2008) were described previously.

Cell Culture, Transfection, and Biochemical Analysis

Hsp47$^{+/+}$ (WT) and *Hsp47*$^{-/-}$ (KO-11 and KO-13) mouse embryonic fibroblasts were reported previously (Nagai *et al.*, 2000). Mov13 cells and Mov13-derived cell lines (see Supplemental Figure S1) were also reported previously (Lamande and Bateman, 1993; Fitzgerald *et al.*, 1999). Cells were cultured in DMEM supplemented with 10% fetal bovine serum (FBS), ascorbic acid (50 μg/ml) and antibiotics. Cells were transfected with expression vectors using Lipofectamine LTX (Invitrogen, Carlsbad, CA) according to the manufacturer's instructions. Proteins were extracted from fibroblasts using cell extraction buffer containing 0.05 M Tris-HCl. pH 8.0, 0.15 M NaCl, 5.0 mM EDTA, 1% NP-40, and protease inhibitors [2.0 mM *N*-ethylmaleimide, 2.0 mM 4-(2-aminoethyl)-benzenesulfonyl fluoride, 1 μg/ml leupeptin and pepstatin] at 4°C. After centrifugation (14,000 rpm, 20 min), supernatant (detergent soluble), and pellet (detergent insoluble) fractions were collected and used for Western blot analysis. Determination of protein concentration and Western blotting were performed as previously described (Ishida *et al.*, 2006).

Inhibitors

MG132 (Peptide Institute, Osaka, Japan), lactacystin (Kyowa Medics, Tokyo, Japan), bafilomycin A1 (Wako, Osaka, Japan), E64d (Calbiochem, San Diego, CA), pepstatin A (Sigma, St. Louis, MO), wortmannin (Calbiochem), LY294002 (Calbiochem), rapamycin (Calbiochem), and tunicamycin (Sigma) were purchased from the indicated sources.

Antibodies

Mouse monoclonal antibodies to PDI (Stressgen, Victoria, BC, Canada), GAPDH (HyTest, Turku, Finland), ubiquitin (Zymed Laboratories, San Francisco, CA), CHOP (Santa Cruz Biotechnology, Santa Cruz, CA), GFP (Roche, Indianapolis, IN), and GM130 (BD Transduction Laboratories, Franklin Lakes, NJ) were purchased from the indicated sources. Rabbit polyclonal antibodies against type I collagen (Chemicon International, Temecula, CA), BiP (Affinity BioReagents, Golden, CO), ATG5 (Sigma), LC3 (MBL, Nagoya, Japan), red fluorescent protein (RFP) (MBL), which reacts with mStrawberry, and α1-antitrypsin (DAKO, Glostrup, Denmark) were also purchased from the indicated sources. A rat mAb against LAMP-2 (Santa Cruz), and goat polyclonal antibody against the type I collagen α2(I) chain (Santa Cruz) were obtained from the indicated sources. A rabbit antibody against the C-propeptide of the type I collagen proα1 chain (LF41) (Fisher *et al.*, 1995) was kindly provided by Dr. Larry W. Fisher (National Institutes of Health, Bethesda, MD). Alkaline phosphatase (AP)-conjugated anti-mouse or anti-rabbit IgG (Biosource, Nivelles, Belgium), AlexaFluor488-conjugated anti-mouse, anti-rabbit, or anti-rat IgG, and AlexaFluor546-conjugated anti-mouse or anti-rabbit IgG (Invitrogen) were used as secondary antibodies.

Immunofluorescence Microscopy

Cells were washed in PBS and fixed with 4% (wt/vol) paraformaldehyde (PFA) in PBS for 15 min. After washing three times in PBS, fixed cells were permeabilized with 0.1% (vol/vol) Triton X-100/PBS for 5 min or 50 μg/ml digitonin/PBS for 5 min for LC3 staining. Nonspecific protein binding in permeabilized cells was blocked by incubation with 2% goat serum/PBS for 30 min. After incubation with specific antibodies, cells were incubated with AlexaFluor-conjugated anti-mouse, anti-rabbit, or anti-rat IgG. Fluorescent signals were analyzed by an LSM 510 META confocal laser microscope (Carl Zeiss, Jena, Germany).

Fluorescence Recovery after Photobleaching Analysis

Fluorescence recovery after photobleaching (FRAP) analysis was performed as described previously (Lippincott-Schwartz *et al.*, 2001; Kitamura *et al.*, 2006). Briefly, cells were transfected with GFP-proα1(I) or GFP-ER as a control using Lipofectamine LTX. Before FRAP analysis, culture medium was changed from normal medium to phenol red–free medium containing 25 mM HEPES buffer (Invitrogen). Regions of the ER were bleached using a 488-nm Argon laser at 100% power through a C-Apochromat 40×/1.2 NA Corr. water immersion objective using the LSM 510 META microscope at 37°C. For recovery measurements, GFP was excited with a 488-nm Argon (30 mW) laser at 1% AOTF transmission. Signals were collected through a 505-nm-long path emission filter. In control experiments, cells were fixed in PBS containing 4% (wt/vol) PFA for 1 h.

Immunoelectron Microscopy

Pre-embedding gold-enhanced immunostaining was performed as previously described (Luo *et al.*, 2006). Cryo-ultramicrotomy and double-immunogold staining on the cryo-ultrathin sections were carried out as described previously (Kimura *et al.*, 2008). Antibodies against type I collagen (Chemicon), LAMP-2 (Santa Cruz), GFP (Roche), or LC3 (MBL) were used as primary antibodies.

RNA interference–mediated Knockdown

Cells were transfected with ATG5 siRNA (Invitrogen; oligo ID MSS247019, MSS247020) or nonspecific (NS) small interfering RNA (siRNA; Invitrogen

oligo ID 12935–300) using Lipofectamine RNAiMAX according to the manufacturer's instructions. After culture for 48 h, knockdown efficiency was determined at the RNA and protein levels. Primers used for RT-PCR analysis were GACAAAGATGTGCTTCGAGATGTG (forward) and GTAGCTCAGATGCTCGCTCAG (reverse) for ATG5 and CAGGAGCGAGACCCCACTAA (forward) and GCCTGCTTCACCACCTTCTT (reverse) for GAPDH.

Metabolic Labeling and Immunoprecipitation

Cells were cultured in the presence of 4.1 MBq/ml ^{35}S-labeled Met and Cys (Express ^{35}S Protein Labeling Mixture, PerkinElmer Life Sciences, Boston, MA) containing 10% dialyzed FBS for 20 min. For pulse-chase experiments, labeled cells were chased for appropriate periods of time in medium containing excess unlabeled Met and Cys. Soluble proteins were extracted in cell extraction buffer, and antibody was added to cell extracts or culture media. Immune complexes were captured using protein A-Sepharose (GE Healthcare Bio-Sciences, Piscataway, NJ) and washed in cell extraction buffer. Proteins were extracted in SDS-PAGE sample buffer and separated by SDS-PAGE. Gels were exposed to phosphor-imaging plates and analyzed by a STORM 820 image analyzer (GE Healthcare Bio-Sciences).

Analysis of Cell Death

Apoptotic cell death was analyzed by Hoechst33342 staining as previously described (Ogata *et al*., 2006). Cell counting was performed using a Biozero digital microscope (Keyence, Osaka, Japan) equipped with a PlanFluor 20×, 0.50 NA objective (Nikon, Tokyo, Japan).

Statistical Analysis

Significant differences were determined by Student's *t* test.

RESULTS

Lysosomal Degradation of Misfolded Procollagen in Hsp47-disrupted Cells

We previously reported using Hsp47-disrupted mouse embryos and fibroblasts that type I procollagen accumulates as detergent-insoluble form in the ER because of failure to form a properly folded triple helix (Marutani *et al*., 2004; Ishida *et al*., 2006). FRAP analysis revealed that the fluorescence recovery of GFP-proα1(I) in the ER of *Hsp47*$^{-/-}$ cells decreased (~65%) relative to that of *Hsp47*$^{+/+}$ cells (~90%; Figure 1, A and B, and Supplemental Figure S2A), whereas fluorescence recovery of GFP-ER, a control GFP expressed in the ER, was similar in both cell lines (Supplemental Figure S2, B–D). To examine whether this delay in fluorescence recovery was due to aggregate formation of procollagen in the ER of *Hsp47*$^{-/-}$ cells, we performed a centrifugal fractionation assay followed by immunoblotting. Collagen synthesis and the level of accumulated procollagen increased when the culture became confluent, and therefore cells from confluent cultures on the third day of culture were used for the assay. Figure 1C shows that procollagens increased in the detergent-insoluble fraction of *Hsp47*$^{-/-}$ cells but not in the detergent-insoluble fraction of *Hsp47*$^{+/+}$ cells. These data strongly suggested that procollagen accumulates as immobile and detergent-insoluble aggregates in *Hsp47*$^{-/-}$ cells.

To investigate how the misfolded procollagen is eliminated from the ER, we examined possible involvement of two major degradation systems, the ubiquitin–proteasome (Hershko *et al*., 2000) and ubiquitin–lysosome (Luzio *et al*., 2007; Mizushima *et al*., 2008) systems. In the presence of the proteasome inhibitors, MG132 and lactacystin, overall polyubiquitination of intracellular proteins was significantly increased, indicating that these inhibitors work effectively (Supplemental Figure S3A). Under these conditions, however, procollagen accumulation was unaffected either in *Hsp47*$^{+/+}$ or *Hsp47*$^{-/-}$ cells (Figure 1D and Supplemental Figure S3A). In contrast, inhibition of lysosome-mediated degradation by E64d and pepstatin A, inhibitors of lysosomal proteases including the cathepsins (Komatsu *et al*., 2007b), or bafilomycin A1, a V-ATPase inhibitor (Yoshimori *et al*., 1991), significantly enhanced the accumulation of insoluble procollagen in *Hsp47*$^{-/-}$ cells, but not in *Hsp47*$^{+/+}$ cells (Figure 1E and Supplemental Figure S3B). Pulse-chase experiments followed by immunoprecipitation demonstrated that degradation of newly synthesized procollagen was inhibited by bafilomycin A1, but not by lactacystin in *Hsp47*$^{-/-}$ cells (Figure 1G). In contrast, newly synthesized procollagen in *Hsp47*$^{+/+}$ cells was secreted very rapidly as described previously (Ishida *et al*., 2006), and the rate was not affected by bafilomycin A1 or lactacystin (Figure 1F). These data clearly indicate that misfolded procollagen that accumulates in the ER due to the absence of Hsp47 is degraded by lysosomal enzymes, but not by the proteasome.

Procollagen is localized primarily in the Golgi apparatus in *Hsp47*$^{+/+}$ cells, as indicated by colocalization with GM130 (Golgi marker) but not PDI (ER marker; Figure 2, A and B). However, procollagen in *Hsp47*$^{-/-}$ cells was localized in the ER (Figure 2, D and E), as we previously reported (Ishida *et al*., 2006). In the presence of E64d/pepstatin A, procollagen in *Hsp47*$^{-/-}$ cells accumulated in lysosomes, as indicated by colocalization with LAMP-2, a lysosome marker (Figure 2F). In contrast, colocalization of procollagen with LAMP-2 was not observed in *Hsp47*$^{+/+}$ cells even in the presence of E64d/pepstatin A (Figure 2C). It was previously reported that autophagosomes fuse with endocytotic structures such as multivesicular bodies (MVBs) to generate the amphisome, which then fuses with lysosomes (Filimonenko *et al*., 2007; Fader and Colombo, 2009). Immunoelectron microscopy revealed that procollagen in *Hsp47*$^{-/-}$ cells was located in amphisome-like structures (Figure 2G). Localization of procollagen in LAMP-2-positive vesicular structures was observed by double labeling immunoelectron microscopy in *Hsp47*$^{-/-}$ cells after E64d/pepstatin A treatment (Figure 2, H and I). These results suggest that misfolded procollagen is delivered to the lysosome via amphisome-like structures for degradation in *Hsp47*$^{-/-}$ cells.

Autophagy Is Activated in Hsp47-Null Cells

Recently, aggregation prone proteins in the ER were reported to be degraded through autophagy as well as ERAD (Vembar and Brodsky, 2008). To test whether the lysosome-dependent degradation of misfolded collagen in *Hsp47*$^{-/-}$ cells is mediated by autophagy, we examined the activation of LC3, an autophagy marker (Klionsky *et al*., 2008). LC3 is a microtubule associated protein existing as two isoforms, LC3-I and LC3-II, in vivo. Posttranslational modification with phosphatidylethanolamine (PE) converts LC3-I to LC3-II. The LC3-II form is active in autophagosome formation and binds to the autophagosome membrane (Kabeya *et al*., 2000). Immunoblotting experiments of cell extracts indicated that LC3-II was induced in *Hsp47*$^{-/-}$ cells, but not in *Hsp47*$^{+/+}$ cells (Figure 3A). The level of LC3-II in *Hsp47*$^{-/-}$ cells increased when cells were treated with lysosomal inhibitors (Figure 3B). Immunostaining of endogenous LC3 revealed a large number of strongly stained punctate structures in *Hsp47*$^{-/-}$ cells (Figure 3C), similar to a typical autophagosome staining patterns. In contrast, a weak, diffuse cytoplasmic staining pattern was observed in *Hsp47*$^{+/+}$ cells. Immunoelectron microscopy indicated that vesicular structures surrounded by LC3-positive membranes were formed in *Hsp47*$^{-/-}$ cells (Figure 3D). GFP-LC3 colocalized with the membrane of early-autophagosomal structures (Figure 3E) when transiently transfected into *Hsp47*$^{-/-}$ cells. Moreover, colocalization of procollagen and LC3 was observed *Hsp47*$^{-/-}$ cells (Figure 3F). Taken together, these data strongly suggest that autophagy is strongly induced, and a

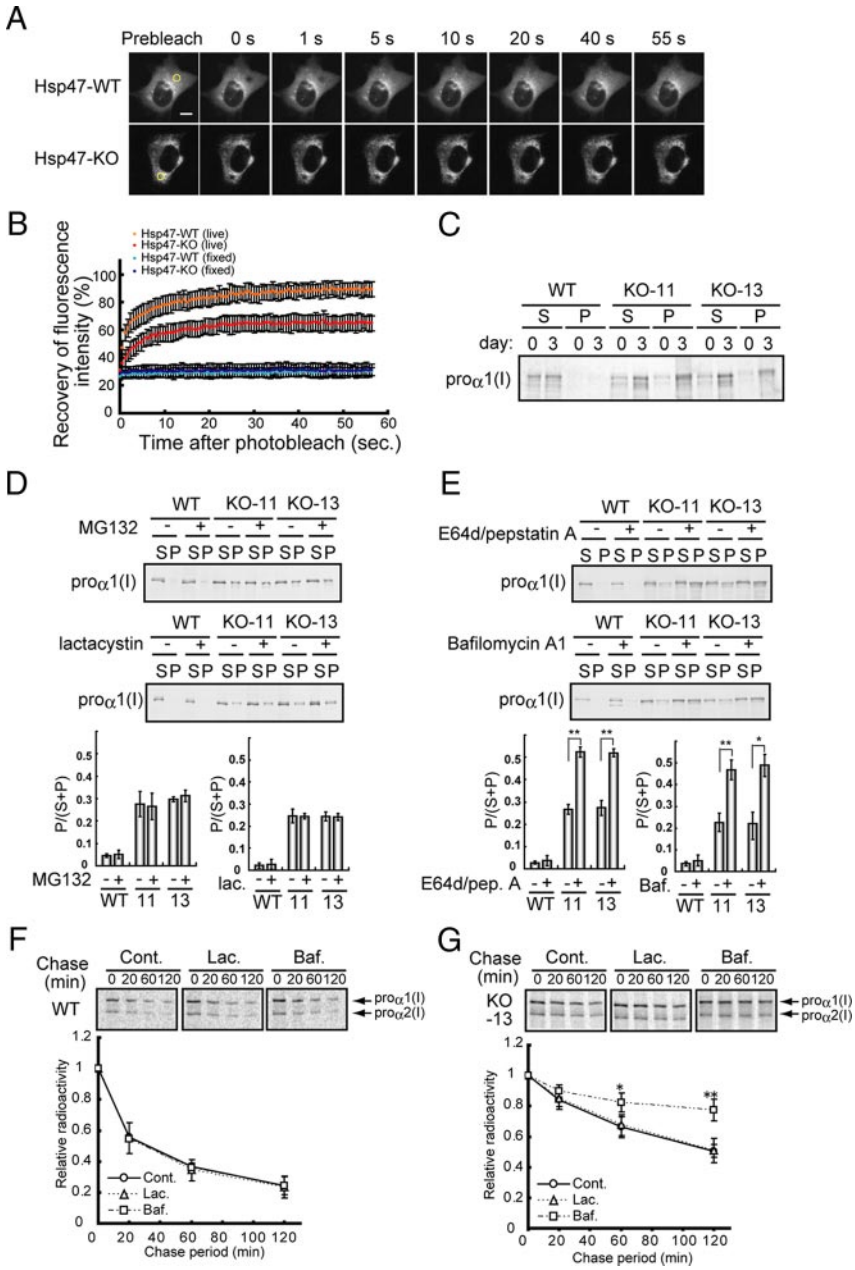

Figure 1. Inhibition of lysosomes, but not of proteasomes, stimulates accumulation of misfolded collagen in *Hsp47*$^{-/-}$ cells. (A) FRAP analysis of type I collagen in *Hsp47*$^{+/+}$ and *Hsp47*$^{-/-}$ (KO-13) cells. Cells were transfected with the GFP-proα1(I) expression vector. A region of the ER was photobleached and after recovery fluorescence intensity was recorded. Bar, 10 μm. (B) Quantification of fluorescence intensity during FRAP analysis (n = 20). (C) Solubility of type I collagen in *Hsp47*$^{+/+}$ and *Hsp47*$^{-/-}$ cells was analyzed by centrifugal fractionation (14000 rpm, 20 min) followed by Western blotting with anti-proα1(I) collagen (LF-41) antibody. Two independent fibroblastic cell lines derived from *Hsp47*$^{-/-}$ mouse embryos (KO-11 and KO-13) were used. S, supernatant; P pellet. (D and E) Accumulation of type I collagen in detergent-soluble and -insoluble fractions after treatment with proteasome (D) or lysosome (E) inhibitors for 12 h. Cells were treated with 2 μM MG132 and 5 μM lactacystin (D), 10 μg/ml E64d/pepstatin A and 100 nM bafilomycin A1 (E). Band intensities in supernatant and pellet fractions were quantified and the pellet/(supernatant plus pellet) ratio was estimated; means $\pm$ SDs are shown for three independent experiments. (F and G) Newly synthesized procollagen in *Hsp47*$^{-/-}$ cells is degraded by the lysosome pathway, but not by the proteasome pathway. *Hsp47*$^{+/+}$ (F) and KO-13 *Hsp47*$^{-/-}$(G) cells were pulse labeled with ^{35}S-labeled Met and Cys for 15 min and chased with unlabeled amino acids for the indicated times in the presence of 10 μM lactacystin or 100 nM bafilomycin A1, or in their absence as a control. Cell lysates were analyzed by immunoprecipitation with anti-type I collagen antibody (Chemicon) followed by SDS-PAGE. The radioactivity of each band was quantified (n = 3). *$p < 0.05$; **$p < 0.01$.

large number of autophagosomes that contain type I procollagen aggregates are produced in *Hsp47*$^{-/-}$ cells.

Inhibition of Autophagy Stimulates Accumulation of Misfolded Procollagen and Cell Death

To examine whether autophagic activity in *Hsp47*$^{-/-}$ cells is required for the clearance of misfolded procollagen in the ER, cells were treated with inhibitors of autophagic activity, namely wortmannin and LY294002. These substances inhibit autophagosome formation by inhibiting phosphatidylinositol 3′-kinase activity (Blommaart *et al.*, 1997). Treatment of *Hsp47*$^{-/-}$ cells with these inhibitors significantly enhanced the accumulation of procollagen in insoluble fractions (Figure 4A). We also examined the effect of rapamycin, which induces autophagy by inhibiting mTor (Berger *et al.*, 2006). Stimulation of autophagic activity by rapamycin treatment clearly decreased the accumulation of procollagen in the insoluble fraction of *Hsp47*$^{-/-}$ cells (Figure 4B). These results indicate that misfolded procollagen is eliminated through autophagy in *Hsp47*$^{-/-}$ cells.

ATG5 is an essential factor for autophagosome formation (Mizushima *et al.*, 2001). To examine whether depletion of the essential factor affects degradation of procollagen accumulated in the ER of *Hsp47*$^{-/-}$ cells, endogenous ATG5 level was reduced by RNA interference (RNAi)-mediated knockdown. Specific siRNA effectively decreased levels of ATG5 mRNA (Figure 4C) and ATG5 protein complexed with ATG12 (Mizushima *et al.*, 2001; Figure 4D). Activation of autophagy was almost completely inhibited by ATG5 knockdown, as examined by LC3-II levels (Figure 4E). Under the ATG5 knockdown conditions, inhibition of autophagic activity significantly enhanced the accumulation of insoluble procollagen in *Hsp47*$^{-/-}$ cells, but not in *Hsp47*$^{+/+}$ cells (Figure 4F). Overexpression of an ATG4B mutant,

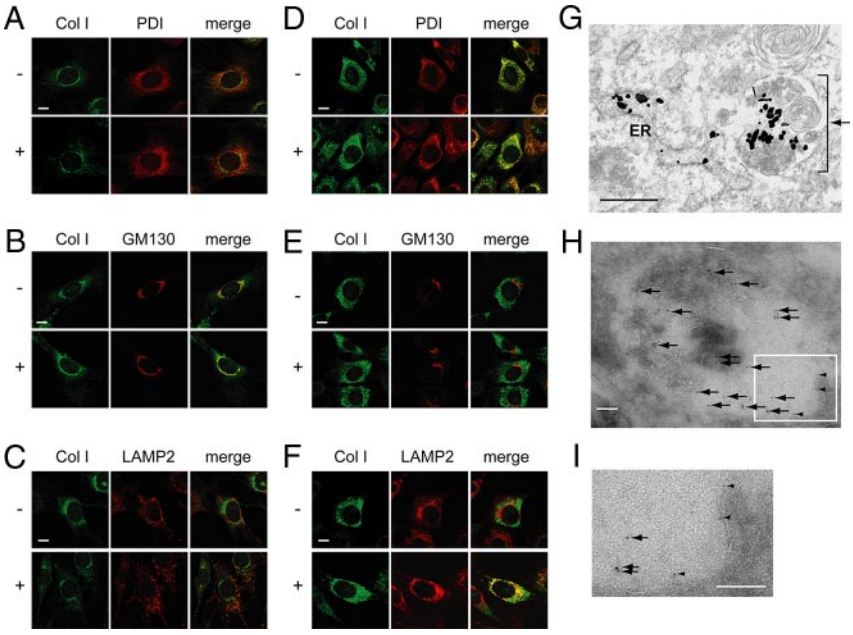

Figure 2. Inhibition of lysosomal degradation in *Hsp47*$^{-/-}$ cells results in accumulation of collagen in lysosomes. *Hsp47*$^{+/+}$ (A–C) and *Hsp47*$^{-/-}$ (KO-13) cells (D–F) were cultured in the presence (+) or absence (−) of E64d/pepstatin A. Localization of type I collagen was analyzed by double staining with antibodies against localization marker proteins. PDI (A and D), GM130 (B and E) and LAMP2 (C and F) were used as ER, Golgi, and lysosome markers, respectively. Bar, 10 μm. (G) Preembedding immunoelectron microscopic observation of type I collagen in *Hsp47*$^{-/-}$ cells under lysosome inhibition conditions. Cells were treated with E64d/pepstatin A. An arrow indicates amphisomes-like structures. Bar, 500 nm. (H) Double-labeling immunoelectron microscopy of type I collagen and LAMP-2 in *Hsp47*$^{-/-}$ cells. Type I collagen and LAMP-2 are labeled with gold particles of 10 nm (arrows) and 5 nm (arrowheads), respectively. (I) A high-magnification view of the region boxed in H. Bar, 100 nm.

which forms stable complex with LC3-I and efficiently inhibits autophagy-mediated degradation (Fujita *et al.*, 2008), also stimulated accumulation of insoluble procollagen in *Hsp47*$^{-/-}$ cells (Figure 4G). These results clearly indicate that degradation of misfolded procollagen in *Hsp47*$^{-/-}$ cells is highly dependent on autophagic activity.

To analyze whether the autophagy-mediated clearance stimulated in *Hsp47*$^{-/-}$ occurs randomly from the ER, the level of PDI, a soluble ER protein, was examined under ATG5-knockdown conditions. In contrast to the significant increase in the intracellular procollagen level, particularly in pellet fractions (Figure 4F), the level of PDI was unaffected by ATG5-knockdown (Supplemental Figure S4). BiP, which associates with unfolded/misfolded procollagen in the ER, also accumulated in the detergent-insoluble fraction with procollagen in *Hsp47*$^{-/-}$ cells after inhibition of autophagy (Supplemental Figure S4). Thus, degradation of insoluble procollagen would appear not to be performed by the random elimination of the ER, suggesting that some mechanism must exist for the selective clearance of the ER containing aggregated proteins.

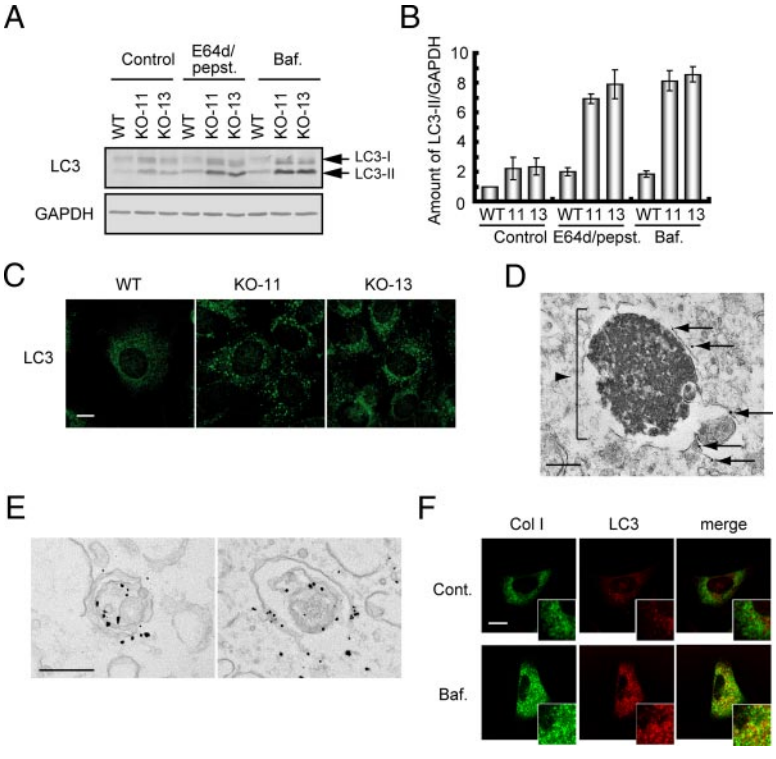

Figure 3. Autophagy is induced in *Hsp47*$^{-/-}$ cells. (A) Western blot analysis of LC3 in *Hsp47*$^{-/-}$ cells in the presence or absence of lysosomal inhibitors. Note that LC3-II is the membrane bound form. (B) Quantification of LC3-II (n = 3). (C) Immunofluorescence staining of endogenous LC3. Bar, 10 μm. (D) Preembedding immunoelectron microscopic observation of LC3 localization in *Hsp47*$^{-/-}$ cells treated with E64d/pepstatin A. Gold-enhanced gold particles showing the presence of LC3 (arrows) are localized on the membrane of an autophagosome (an arrowhead) fusing with lysosome. Bar, 500 nm. (E) Preembedding immunoelectron microscopic observation of LC3 localization. GFP-LC3 was expressed in *Hsp47*$^{-/-}$ (KO-13) cells and analyzed with anti-GFP antibody. Bar, 200 nm. (F) Double staining of type I collagen and endogenous LC3 in *Hsp47*$^{-/-}$ (KO-13) cells cultured in the presence or absence of 100 nM bafilomycin A1 for 6 h. Bar, 10 μm.

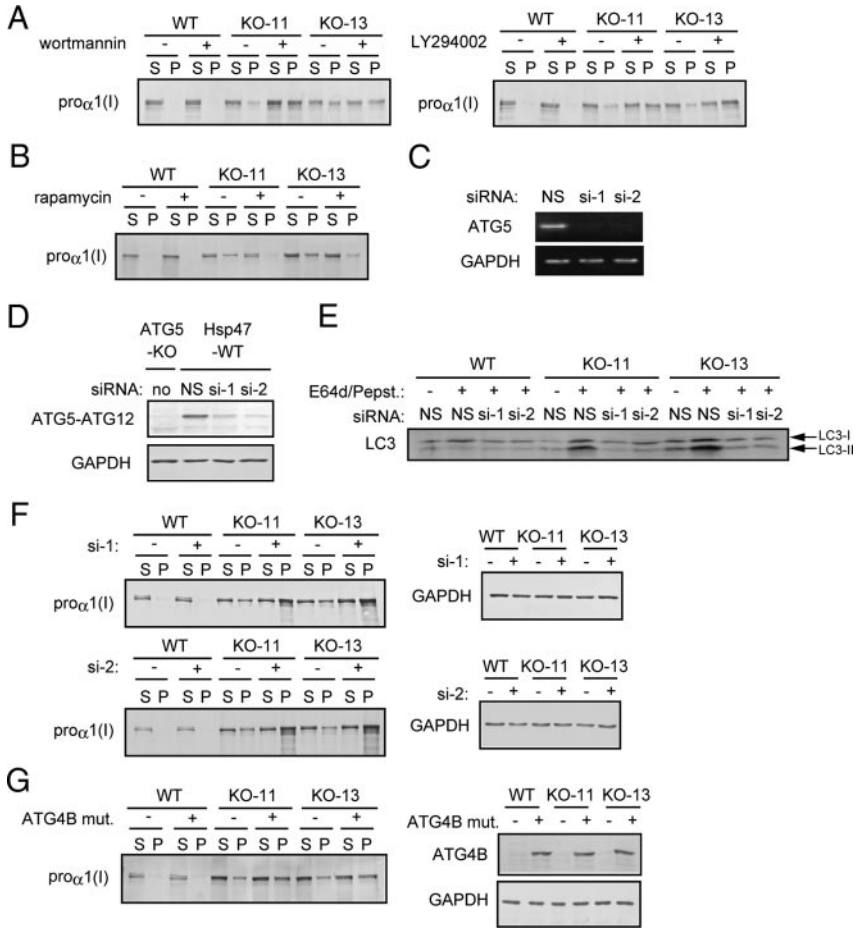

Figure 4. Autophagy plays a critical role in the clearance of misfolded procollagen in *Hsp47*$^{-/-}$ cells. (A) Autophagy inhibitors stimulated the accumulation of procollagen in the detergent-insoluble fraction of *Hsp47*$^{-/-}$ cells. *Hsp47*$^{+/+}$ and *Hsp47*$^{-/-}$ cells were treated with 5 nM wortmannin (left panel) or 5 μM LY294002 (right panel) for 4 h, and cell lysates were analyzed by centrifugal fractionation (14,000 rpm, 20 min) followed by Western blot analysis with anti-proα1(I; LF-41) antibody. S, supernatant; P, pellet. (B) An autophagy activator alleviates the accumulation of detergent-insoluble procollagen in *Hsp47*$^{-/-}$ cells. Cells were treated with 10 μg/ml rapamycin for 6 h. (C–F) Knockdown of ATG5 stimulates the accumulation of insoluble collagen in *Hsp47*$^{-/-}$ cells. Cells were transiently transfected with ATG5 siRNA or nonspecific (NS) siRNA. (C) Total RNA was extracted after culture for 48 h and analyzed by RT-PCR using ATG5 and GAPDH-specific primers. (D) ATG5 protein levels were analyzed by Western blotting. Lysates from ATG5-knockout (KO) cells were used as a control. (E) LC3 protein levels were determined after RNAi-mediated ATG5 knockdown in the presence or absence of E64d/pepstatin A. (F) type I collagen was analyzed by centrifugal fractionation followed by Western blotting with anti-proα1(I) (LF-41) antibody after RNAi-mediated ATG5 knockdown. (G) Accumulation of insoluble procollagen is enhanced by an inactive ATG4B mutant that inhibits autophagy activation. Cells were transfected with an ATG4B mutant fused to mStrawberry, and levels of type I collagen and ATG4B proteins were analyzed by Western blot analysis with anti-proα1(I) (LF-41) and anti-RFP antibodies.

Accumulation of misfolded proteins in the ER is potentially toxic to the cell, and apoptotic cell death was previously observed in *Hsp47*$^{-/-}$ embryos (Marutani *et al.*, 2004). To test whether autophagic activity contributes to cell survival under conditions that misfolded procollagens are aggregated in the ER, apoptotic cell death in *Hsp47*$^{-/-}$ cells was determined in the presence or absence of ATG5 siRNA. Inhibition of autophagy by ATG5 knockdown significantly increased apoptotic cell death in *Hsp47*$^{-/-}$ cells, but not in *Hsp47*$^{+/+}$ cells (Figure 5, A and B). Under the same conditions, up-regulation of CHOP expression was observed only in *Hsp47*$^{-/-}$ cells (Figure 5, C and D). Apoptotic cell death induced by ER stress is known to be mediated by up-regulation of ATF4, and this transcription factor induces CHOP expression and activation of caspase-3 and caspase-12. Thus, we examined levels of ATF4, caspase-3, and caspase-12 in *Hsp47*$^{-/-}$ cells and confirmed that all three factors are up-regulated (Ishida, Kubota, and Nagata, unpublished results). These data suggest that ER stress caused by the accumulation of misfolded procollagen induces apoptosis via the ATF4-CHOP pathway. Taken together, these observations clearly indicate that autophagy protects cells against the toxic effects of procollagen aggregates accumulated in the ER.

Autophagy-dependent Degradation of Disease-causing Mutants of Type I Collagen

Type I collagen is composed of two proα1(I) chains and one proα2(I) chain, in which mutations cause brittle-bone diseases including OI (Marini *et al.*, 2007). In cells derived from OI patients, procollagen is misfolded and accumulates in the ER (Kojima *et al.*, 1998). However, the mechanism of degradation of these misfolded procollagen molecules is largely unknown. We therefore examined the role of autophagy in the degradation of mutant collagen using cultured Mov13 cells, in which the proα1 chain of type I collagen is not expressed due to a retroviral insertion in the first intron of the gene, resulting in expression of only the proα2(I) chain (Schnieke *et al.*, 1983; Breindl *et al.*, 1984). We first examined proα2(I) chain degradation in Mov13 cells and found that it is degraded via the lysosomal pathway, as indicated by the effect of lysosomal inhibitors (Figure 6A). Proteasome inhibitors did not inhibit proα2(I) chain degradation in Mov13 cells, consistent with a previous report (Gotkin *et al.*, 2004). Because this degradation was inhibited by the treatment of cells with brefeldin A, proα2(I) chain in Mov13 cells is assumed to be degraded via COPII pathway. Next, we examined the involvement of autophagy in the clearance of the proα2(I) chain. Although the LC3-II level increased slightly in the presence of lysosomal inhibitors (Figure 6B), ATG5 knockdown or the overexpression of an inactive ATG4B mutant had no significant effect on proα2(I) chain accumulation (Figure 6, C and D). Thus, the proα2 chain of type I collagen appears to be degraded in lysosomes via an autophagy-independent pathway in Mov13 cells.

Several Mov13-derived cell lines that were stably transfected with the wild-type α1 chain or disease-causing mutants of type I collagen proα1 chains have been established (Lamande and Bateman, 1993; Fitzgerald *et al.*, 1999). In this

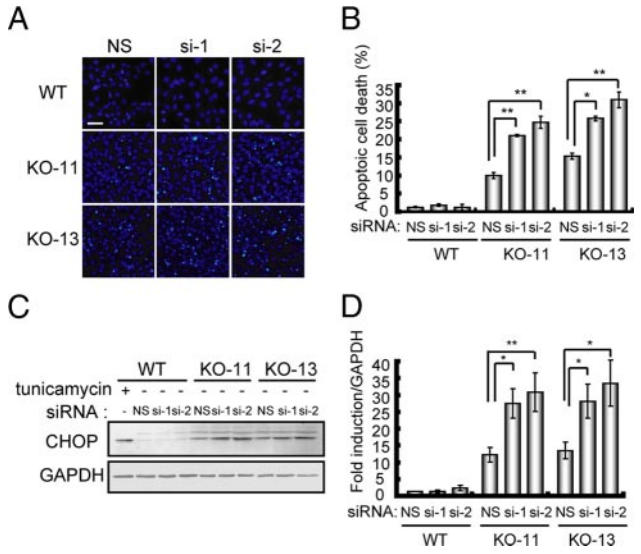

Figure 5. Inhibition of autophagic activity stimulates ER-stress–induced apoptotic cell death in *Hsp47*$^{-/-}$ cells. (A) Cells were treated with siRNAs for ATG5 or nonspecific siRNA as a control. Cells were stained with Hoechst 33342 to visualize DNA condensation, an indication of apoptotic cell death. Bar, 50 μm. (B) Number of apoptotic cells under ATG5 knockdown conditions (n = 4). (C) Western blot analysis of CHOP. Tunicamycin (5 μg/ml) was used as a control for ER stress conditions. (D) Quantification of CHOP levels (n = 3). *p < 0.05; **p < 0.01.

study, we used three of these cell lines (Supplemental Figure S1): Mov13-WT, Mov13-Arg, and Mov13-IAFS cells. In Mov13-Arg cells, Gly859 of the proα1(I) chain, which is located in the triple helix-forming region, is mutated to Arg. In Mov13-IAFS cells, the mutation is located in the C-propeptide region of the proα1(I) chain [a five-base pair deletion at the carboxy terminus, resulting in extension of

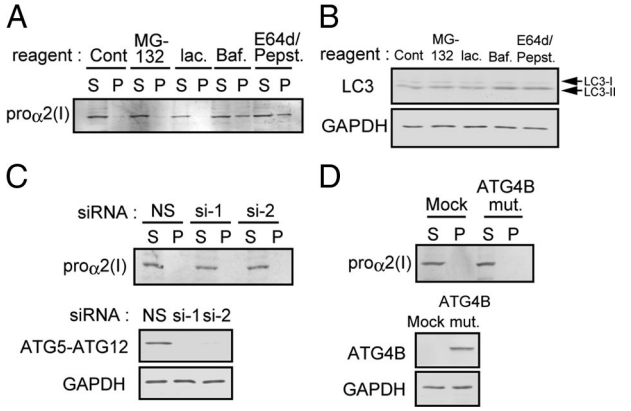

Figure 6. type I collagen proα2 chain in Mov13 cells is degraded by an autophagy-independent lysosomal pathway. (A) Solubility of the type I collagen proα2 chain was examined by Western blotting after treatment with the indicated inhibitors. S, supernatant; P, pellet. (B) LC3 levels were analyzed by Western blotting after treatment with the indicated inhibitors. (C) Solubility of the proα2 chain of type I collagen was analyzed after ATG5-knockdown (top panel). ATG5 and GAPDH proteins in Mov13 cells were examined by Western blotting after knockdown of ATG5 (bottom and middle panels). (D) Solubility of the proα2 chain was analyzed after ATG4B mutant overexpression (top panel). Expression level of ATG4B and GAPDH was examined by Western blotting (bottom panel).

the proα1(I) chain] and causes a defect in trimer formation. The proα1(I) chain of this C-propeptide mutant was reported to be degraded via the ERAD pathway (Fitzgerald *et al.*, 1999). We confirmed that in Mov13-WT cells, the exogenously introduced proα1(I) chain and the endogenous proα2(I) chain were correctly folded and secreted into the medium, whereas neither of the chains were secreted from Mov13-Arg or Mov13-IAFS cells (Supplemental Figure S5), probably as a result of misfolding (Lamande and Bateman, 1993; Fitzgerald *et al.*, 1999).

Nonreducing SDS-PAGE followed by immunoblotting indicated that type I collagen forms trimers in Mov13-Arg cells as well as in Mov13-WT cells (Figure 7A). In contrast, type I collagen in Mov13-IAFS cells failed to form trimers (Figure 7A). We analyzed the degradation of procollagen in these cell lines using lysosome or proteasome inhibitors. Accumulation of type I collagen proα1 and proα2 chains was unaffected by the presence of proteasome or lysosome inhibitors in Mov13-WT cells (Figure 7B, top panel, and Supplemental Figure S6A). In Mov13-IAFS cells, inhibition of proteasome activity significantly stimulated accumulation of the proα1(I) chain, particularly in the supernatant fraction (Figure 7B, middle panel, and Supplemental Figure S6A) concomitant with the induction of polyubiquitination of the proα1(I) chain (Figure 7C). These results confirm that the proα1(I) chain is degraded by ERAD in the timer formation–deficient cells. The accumulation of the proα2(I) chain in the insoluble fractions of Mov13-IAFS cells increased in the presence of lysosome inhibitors, but not in the presence of proteasome inhibitors (Figure 7B, middle panel, and Supplemental Figure S6A). These results are consistent with the data from untransfected Mov13 cells (Figure 6), and are reasonable because the proα1(I) and proα2 (I) chains cannot form timers in Mov13-IAFS cells because of the proα1(I) chain mutation in the trimer-forming C-propeptide region.

In contrast, both the proα1(I) and proα2(I) chains in Mov13-Arg cells are accumulated in insoluble fractions after treatment with lysosome inhibitors, whereas such accumulation was not observed by the treatment with proteasome inhibitors (Figure 7B, bottom panel, and Supplemental Figure S6A). These data suggest that, when misfolded procollagen molecules form trimers as was also seen in *Hsp47*$^{-/-}$ cells, they cannot be eliminated by ERAD, but by autophagy–lysosome system (Figures 1 and 4). In the presence of lysosome inhibitors, the LC3-II level in Mov13-Arg cells was more than fivefold greater relative to that in Mov13-WT cells (Supplemental Figure S6B), indicating that autophagy is induced in Mov13-Arg cells. LC3-II level was not increased by the presence of lysosome inhibitors in Mov13-IAFS cells, consistent with the degradation of this mutant of the proα1(I) chain via ERAD.

We also examined the accumulation of proα1(I) chains in the three Mov13-derived cell lines under ATG5 knockdown conditions. Depletion of ATG5 significantly enhanced accumulation of the proα1(I) and proα2(I) chains in insoluble fractions in Mov13-Arg cells, in which the α1 and α2 chains form misfolded trimers (Figure 7D, right panels, and Supplemental Figure S6C). In contrast, levels of the proα1(I) and proα2(I) chains were unaffected by ATG5 knockdown in Mov13-WT and Mov13-IAFS cells (Figure 7D, left and middle panels, and Supplemental Figure S6C). In the presence of bafilomycin A1, trimeric procollagens accumulated mainly in the insoluble fractions of Mov13-Arg cells as analyzed by nonreducing SDS-PAGE followed by Western blot analysis, suggesting that insoluble procollagen aggregates are mainly composed of misfolded trimeric procollagen instead of misfolded monomeric procollagen (Figure 7E). These results

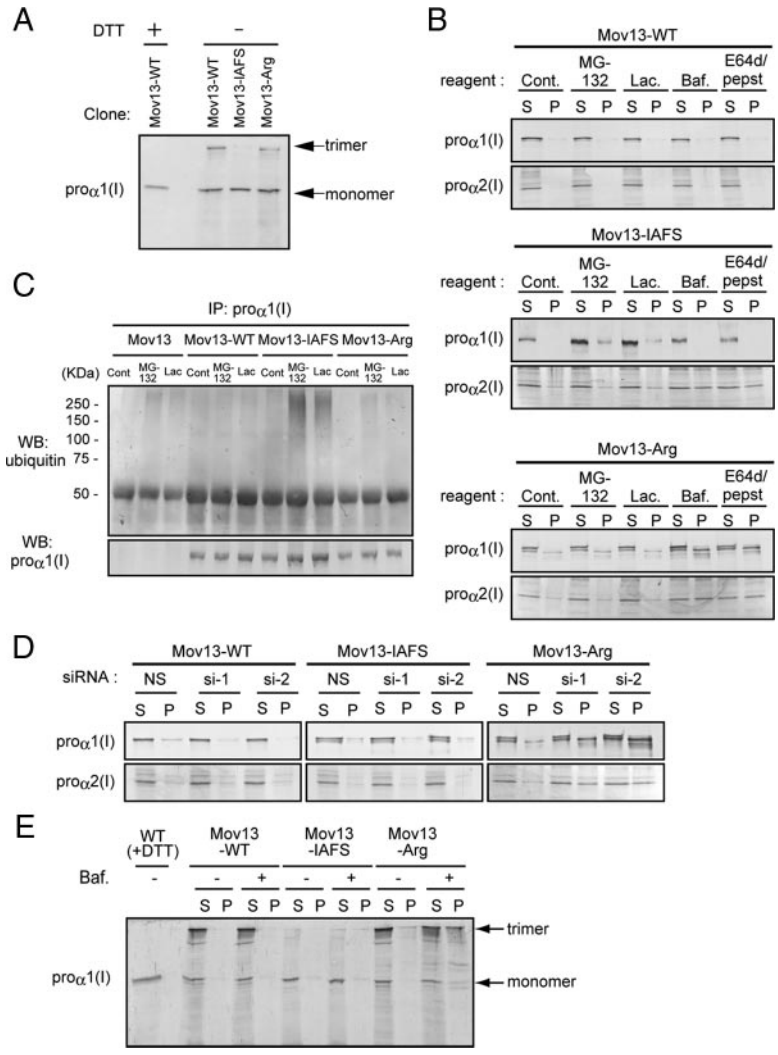

Figure 7. Misfolded trimeric type I collagen is degraded by an autophagic-lysosomal pathway. (A) Collagen trimerization was analyzed by SDS-PAGE under nonreducing conditions followed by Western blotting with anti-proα1(I) (LF-41) antibody. (B) Mov13-derived cell lines were analyzed by Western blotting with antibodies against the proα1(I) and proα2(I) chains of type I collagen after treatment with proteasome or lysosome inhibitors. Mov13-WT cells carry the wild-type proα1 chain of type I collagen. Mov13-IAFS and Mov13-Arg cell lines carry proα1 chain mutations occurring in the C-propeptide and triple helix regions, respectively. S, supernatant; P, pellet. (C) Examination of polyubiquitination of type I collagen in Mov13 cells. Type I collagen proα1 chain was collected by immunoprecipitation and analyzed by Western blotting with antibodies against ubiquitin or proα1(I). (D) Solubility of the proα1(I) and proα2 (I) chains was examined by Western blotting. (E) The trimeric form of procollagen in Mov13-Arg cells increased in the detergent-insoluble fractions after treatment with bafilomycin A1. Cells were treated with or without bafilomycin A1 as a control, and SDS-PAGE was performed under nonreducing conditions followed by Western blot analysis with anti-α1(I) antibody.

thus support the notion that the endogenous autophagic activity is essential for the clearance of ERAD-ineffective aggregates of trimeric procollagen from the ER.

We finally tested whether the ERAD of soluble misfolded proteins is affected by the presence of misfolded procollagen aggregates, which are being eliminated by autophagy from the ER. Mov13-Arg cells were transfected with the NHK variant of α1-antitrypsin, a well-known ERAD substrate (Liu *et al.*, 1999), and degradation of NHK through ERAD was examined by pulse-chase experiments. The degradation of NHK was unaffected by the presence of ATG5 siRNA (Figure 8A). In contrast, lactacystin clearly inhibited the degradation of NHK both in ATG5 siRNA-treated and untreated cells (Figure 8B). These results clearly demonstrated that the elimination of soluble misfolded protein via ERAD and insoluble misfolded protein via autophagy occurs simultaneously and independently within the same cell, and suggest that the autophagy-dependent aggregate elimination system may mainly use factors unrelated to ERAD although detailed mechanisms remain to be investigated.

DISCUSSION

We previously reported using Hsp47-disrupted mouse embryos and cultured cells that type I and type IV procollagens accumulate in the ER due to inability to form properly folded triple helix (Nagai *et al.*, 2000; Marutani *et al.*, 2004; Matsuoka *et al.*, 2004; Ishida *et al.*, 2006). In these embryos and cells, detergent-insoluble procollagens are accumulated in the ER. Thus, the Hsp47-null cells were adopted as a useful model to analyze the fate of aggregated procollagens without genetic mutations (Figures 1–5). In addition, we used Mov13-derived cell lines as models for improperly assembled/folded procollagen because of the genetic mutations (Figures 6 and 7). Type I collagen is a trimer of two α1 chains and one α2 chain. In Mov13 cells, which lacks collagen proα1(I) chain expression (Schnieke *et al.*, 1983; Breindl *et al.*, 1984), the proα2(I) chain is rapidly degraded by the lysosome (Gotkin *et al.*, 2004), which was confirmed in the present study. By reintroducing normal or mutant proα1(I) chains into Mov13 cells, the assembly (trimer formation) and triple helix formation of the α chains can be analyzed. The transfected wild-type proα1(I) chain and endogenous proα2(I) chain in Mov13-WT cells make properly folded trimers and the procollagen is secreted into the medium. The proα1(I) chain in Mov13-IAFS cells cannot make trimers with the endogenous proα2(I) chain because of the mutation in the trimer-forming region, and the α1 chain in Mov13-Arg cells makes an improperly folded trimer. In Mov13-IAFS cells, each proα chain accumulates as a monomer, whereas

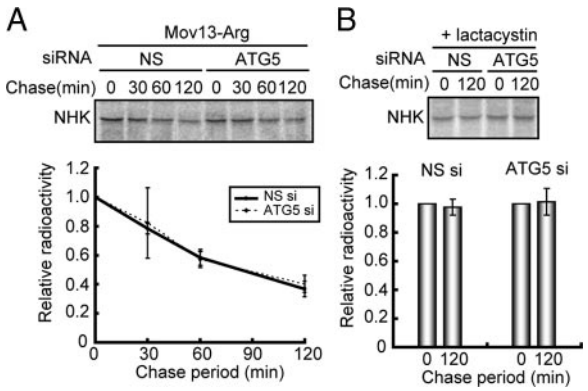

Figure 8. Misfoled procollagen accumulated in the ER does not perturb ERAD activity. Degradation of α1-antitrypsin Null Hong Kong (NHK) variant was examined after transient transfection into Mov13-Arg cells in the presence of ATG5 siRNA or nonspecific siRNA as a control. (A) Pulse-chase experiment was performed under the indicated conditions. Quantified radioactivity is shown at the bottom (n = 3). (B) A pulse-chase experiment was performed in the presence of lactacystin (10 μM; n = 3).

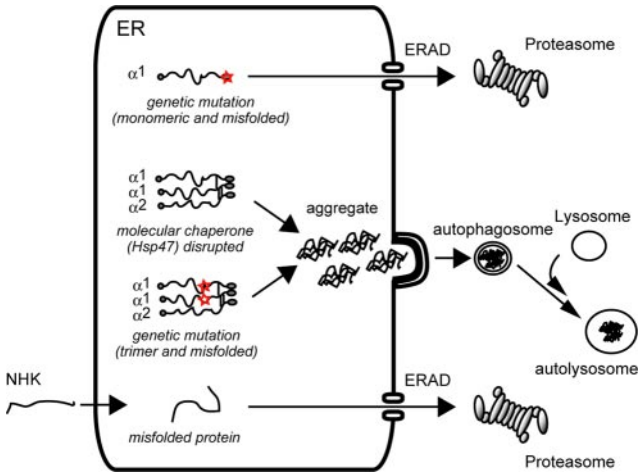

Figure 9. A model for the degradation of misfolded procollagen molecules in the ER. Type I collagen trimers that contain the misfolded proα1(I) chain due to chaperone-disruption or genetic mutation accumulate as aggregates in the ER. These aggregates are eliminated by an autophagy–lysosome pathway, but not by ERAD. In contrast, mutant type I collagen proα1 chain that is deficient in trimer formation is eliminated by the ERAD pathway. In addition, misfolded protein (NHK) and misfolded procollagens are degraded independently by ERAD or autophagy, respectively, in the same cell. Red stars indicate mutated amino acids.

procollagen in Mov13-Arg cells was shown to accumulate in the ER as a detergent-insoluble aggregate, which is similar to that produced in *Hsp47*$^{-/-}$ cells without any mutations in the collagen genes. Using these four cell lines, we have determined the fate of each α chain.

Mutations in type I collagen genes are tightly associated with OI (Millington-Ward *et al.*, 2005). The OI-causing G859R mutation used in the present study (Mov13-Arg) is located in the triple helical domain. This mutant proα1(I) chain accumulated in the ER as detergent-insoluble aggregates that were removed by autophagic degradation. In fact, there are only a few mutations known in the C-propeptide that would result in failed assembly. The vast majority of OI mutations are in the helix-forming region, and the mechanism of degradation for these mutations has never been established. To explore therapeutic strategies for collagen-related diseases for which no effective therapies are currently available, it will be important to determine the fate of the misfolded procollagens in vivo, such as type I collagen in OI, type II collagen in chondrodysplasias, and type III collagen in Ehlers-Danlos syndrome.

In the present study, we found that misfolded procollagens in *Hsp47*$^{-/-}$ and Mov13-Arg cells were degraded in the lysosome via an autophagic pathway, but not via the ERAD pathway (Figures 1–5 and 7). Autophagy is essential for degrading aggregated procollagen as indicated by the use of specific inhibitors and RNAi-mediated knockdown. Consistently, elimination of aggregated procollagen was enhanced by activating autophagic activity with rapamycin. We also showed that inhibition of autophagic activity significantly reduced cell viability in *Hsp47*$^{-/-}$ cells (Figure 5), indicating that autophagy plays an essential role in cell survival by removing ERAD-ineffective misfolded procollagen species from the ER. These observations are consistent with the fact that autophagy has a cell protective effect against ER stressors (Ogata *et al.*, 2006). In contrast, the proα1(I) chain in Mov13-IAFS cells cannot form a trimer with the endogenous proα2(I) chain, and the proα1(I) chain monomer was degraded via ERAD. These observations indicate that aggregated procollagen trimers are degraded by the autophagy-lysosome pathway, whereas misfolded monomer proα1 chains are degraded through ERAD (Figure 9). Using these unique systems where monomeric or trimeric misfolded procollagen α chains can be selectively forced to accumulate in the ER, we have established that the elimination of misfolded proteins by autophagy or ERAD is dictated by whether their accumulated forms adopt multimeric or monomeric forms. Our present study strongly supports the previous observation that soluble human the α-antitrypsin Z variant (ATZ) is destined for clearance by ERAD, whereas aggregated ATZ is destined for autophagic clearance (Kruse *et al.*, 2006). It is worthwhile to note that this partitioning system is conserved from yeasts to mammals.

Intriguingly, the proα2(I) chain in Mov13 cells is not degraded through ERAD or autophagy, but by lysosomes via an autophagy-independent pathway (Figure 6). The proα2(I) chain in Mov13 cells is transported to the Golgi apparatus before being degraded in the lysosome (Gotkin *et al.*, 2004), which may suggest the existence of additional components responsible for discriminating misfolded procollagens. However, detailed mechanisms for the third degradation pathway remain to be investigated.

A key question is how the accumulation of aggregation-prone misfolded proteins within the ER triggers autophagy, which is exclusively a cytoplasmic phenomenon. Bernales *et al.* (2006) suggested that ER expansion induced by ER stress could trigger digestion of the ER via autophagy in yeast (Bernales *et al.*, 2006). ER stress was also reported to induce expression of key components required for autophagy in yeast and mammalian cells (Ogata *et al.*, 2006; Yorimitsu *et al.*, 2006). In *Hsp47*$^{-/-}$ cells, we observed dilation of the ER by immunoelectron microscopy (Marutani *et al.*, 2004; Ishida *et al.*, 2006) and induction of the spliced XBP-1 (Ishida, Kubota, and Nagata, unpublished results), indicating activation of the ER stress response. At the same time, the activation of LC3-II was also observed in *Hsp47*$^{-/-}$ cells (Figure 3). Thus, ER stress may be an important inducer of autophagic degradation of ER proteins, including aggregated procollagen, although further investigation is needed to clarify the exact links between ER stress and autophagy.

We examined whether misfolded procollagen accumulated in the ER inhibit ERAD activity by coexpressing the ERAD substrate, NHK, in Mov13-Arg cells where procollagen is degraded through autophagy. We found that NHK is degraded by ERAD even when autophagy is blocked by treating the cells with ATG5 siRNA and that the degradation of NHK was totally inhibited by treatment of the cells with the proteasome inhibitor lactacystin in the presence or absence of siRNA treatment (Figures 8). These results suggest not only that ERAD and autophagy exert their degradative activity independently, but also that there exists some mechanism to discriminate among misfolded proteins in the ER and determine their processing either by ERAD or autophagy. Our experiments here suggest that the molecular conformation, and, in particular, the tendency to form aggregates, may determine which degradation pathway is used.

Whether autophagy engulfs and degrades the ER selectively or nonselectively is also a crucial question. In the ER of *Hsp47*$^{-/-}$ cells, the ER-resident molecular chaperone BiP bound procollagen, accumulated in the detergent-insoluble fraction, and was degraded through autophagy (Supplemental Figure S4). Although accumulation of misfolded collagen trimers was significantly stimulated by inhibition of autophagy by RNAi-mediated knockdown particularly in insoluble fractions (Figure 4, A, F, and G), this inhibition did not affect the level of PDI, a soluble protein in the ER (Supplemental Figure S4). These observations suggest a possible mechanism where aggregate-containing regions of the ER are selectively eliminated by autophagy, and this possibility remains to be investigated in the future.

ACKNOWLEDGMENTS

We thank Dr. Rainer Pepperkok (European Molecular Biology Laboratory, Germany) for providing the GFP-proα1(I) expression vector, Dr. Larry W. Fisher (National Institutes of Health, MD) for the antibody to the type I procollagen α1 chain C-propeptide (LF-41) and Dr. Nobuko Hosokawa (Kyoto University, Japan) for the α1-antitrypsin NHK variant expression vector. We are grateful to Dr. Motoko Naitoh (Kyoto University, Japan) and Dr. Naonobu Fujita (Osaka University, Japan) for technical comments and suggestions. Y.I. and A.K. were supported by fellowships from the Japan Society for the Promotion of Science. K.N. was supported by a Grant-in-Aid for Creative Scientific Research (19GS0314). K.N. and H.K. were supported by a Ground-based Research Program for Space Utilization from the Japan Space Forum. J.B. and S.L. are supported by grants from the National Health and Medical Research Council of Australia.

REFERENCES

Anelli, T., and Sitia, R. (2008). Protein quality control in the early secretory pathway. EMBO J. *27*, 315–327.

Berger, Z., *et al.* (2006). Rapamycin alleviates toxicity of different aggregate-prone proteins. Hum. Mol. Genet. *15*, 433–442.

Bernales, S., McDonald, K. L., and Walter, P. (2006). Autophagy counterbalances endoplasmic reticulum expansion during the unfolded protein response. PLoS Biol. *4*, e423.

Blommaart, E. F., Krause, U., Schellens, J. P., Vreeling-Sindelarova, H., and Meijer, A. J. (1997). The phosphatidylinositol 3-kinase inhibitors wortmannin and LY294002 inhibit autophagy in isolated rat hepatocytes. Eur. J. Biochem. *243*, 240–246.

Breindl, M., Harbers, K., and Jaenisch, R. (1984). Retrovirus-induced lethal mutation in collagen I gene of mice is associated with an altered chromatin structure. Cell *38*, 9–16.

Fader, C. M., and Colombo, M. I. (2009). Autophagy and multivesicular bodies: two closely related partners. Cell Death Differ. *16*, 70–78.

Filimonenko, M., Stuffers, S., Raiborg, C., Yamamoto, A., Malerod, L., Fisher, E. M., Isaacs, A., Brech, A., Stenmark, H., and Simonsen, A. (2007). Functional multivesicular bodies are required for autophagic clearance of protein aggregates associated with neurodegenerative disease. J. Cell Biol. *179*, 485–500.

Fisher, L. W., Stubbs, J. T., 3rd, and Young, M. F. (1995). Antisera and cDNA probes to human and certain animal model bone matrix noncollagenous proteins. Acta Orthop. Scand. Suppl. *266*, 61–65.

Fitzgerald, J., Lamande, S. R., and Bateman, J. F. (1999). Proteasomal degradation of unassembled mutant type I collagen pro-alpha1(I) chains. J. Biol. Chem. *274*, 27392–27398.

Fujita, E., Kouroku, Y., Isoai, A., Kumagai, H., Misutani, A., Matsuda, C., Hayashi, Y. K., and Momoi, T. (2007). Two endoplasmic reticulum-associated degradation (ERAD) systems for the novel variant of the mutant dysferlin: ubiquitin/proteasome ERAD(I) and autophagy/lysosome ERAD(II). Hum. Mol. Genet. *16*, 618–629.

Fujita, N., Hayashi-Nishino, M., Fukumoto, H., Omori, H., Yamamoto, A., Noda, T., and Yoshimori, T. (2008). An Atg4B mutant hampers the lipidation of LC3 paralogues and causes defects in autophagosome closure. Mol. Biol. Cell *19*, 4651–4659.

Gajko-Galicka, A. (2002). Mutations in type I collagen genes resulting in osteogenesis imperfecta in humans. Acta Biochim. Pol. *49*, 433–441.

Gotkin, M. G., Ripley, C. R., Lamande, S. R., Bateman, J. F., and Bienkowski, R. S. (2004). Intracellular trafficking and degradation of unassociated proalpha2 chains of collagen type I. Exp. Cell Res. *296*, 307–316.

Hershko, A., Ciechanover, A., and Varshavsky, A. (2000). Basic Medical Research Award. The ubiquitin system. Nat. Med. *6*, 1073–1081.

Hosokawa, N., Wada, I., Natsuka, Y., and Nagata, K. (2006). EDEM accelerates ERAD by preventing aberrant dimer formation of misfolded alpha1-antitrypsin. Genes Cells *11*, 465–476.

Ishida, Y., Kubota, H., Yamamoto, A., Kitamura, A., Bachinger, H. P., and Nagata, K. (2006). Type I collagen in Hsp47-null cells is aggregated in endoplasmic reticulum and deficient in N-propeptide processing and fibrillogenesis. Mol. Biol. Cell *17*, 2346–2355.

Kabeya, Y., Mizushima, N., Ueno, T., Yamamoto, A., Kirisako, T., Noda, T., Kominami, E., Ohsumi, Y., and Yoshimori, T. (2000). LC3, a mammalian homologue of yeast Apg8p, is localized in autophagosome membranes after processing. EMBO J. *19*, 5720–5728.

Kamimoto, T., Shoji, S., Hidvegi, T., Mizushima, N., Umebayashi, K., Perlmutter, D. H., and Yoshimori, T. (2006). Intracellular inclusions containing mutant alpha1-antitrypsin Z are propagated in the absence of autophagic activity. J. Biol. Chem. *281*, 4467–4476.

Kimura, T., Horibe, T., Sakamoto, C., Shitara, Y., Fujiwara, F., Komiya, T., Yamamoto, A., Hayano, T., Takahashi, N., and Kikuchi, M. (2008). Evidence for mitochondrial localization of P5, a member of the protein disulphide isomerase family. J. Biochem. *144*, 187–196.

Kitamura, A., Kubota, H., Pack, C. G., Matsumoto, G., Hirayama, S., Takahashi, Y., Kimura, H., Kinjo, M., Morimoto, R. I., and Nagata, K. (2006). Cytosolic chaperonin prevents polyglutamine toxicity with altering the aggregation state. Nat. Cell Biol. *8*, 1163–1170.

Klionsky, D. J. (2007). Autophagy: from phenomenology to molecular understanding in less than a decade. Nat. Rev. Mol. Cell Biol. *8*, 931–937.

Klionsky, D. J., *et al.* (2008). Guidelines for the use and interpretation of assays for monitoring autophagy in higher eukaryotes. Autophagy *4*, 151–175.

Kojima, T., Miyaishi, O., Saga, S., Ishiguro, N., Tsutsui, Y., and Iwata, H. (1998). The retention of abnormal type I procollagen and correlated expression of HSP 47 in fibroblasts from a patient with lethal osteogenesis imperfecta. J. Pathol. *184*, 212–218.

Komatsu, M., Ueno, T., Waguri, S., Uchiyama, Y., Kominami, E., and Tanaka, K. (2007a). Constitutive autophagy: vital role in clearance of unfavorable proteins in neurons. Cell Death Differ. *14*, 887–894.

Komatsu, M., *et al.* (2007b). Homeostatic levels of P62 control cytoplasmic inclusion body formation in autophagy-deficient mice. Cell *131*, 1149–1163.

Kruse, K. B., Brodsky, J. L., and McCracken, A. A. (2006). Characterization of an ERAD gene as VPS30/ATG6 reveals two alternative and functionally distinct protein quality control pathways: one for soluble Z variant of human alpha-1 proteinase inhibitor (A1PiZ) and another for aggregates of A1PiZ. Mol. Biol. Cell *17*, 203–212.

Lamande, S. R., and Bateman, J. F. (1993). A type I collagen reporter gene construct for protein engineering studies. Functional equivalence of transfected reporter COL1A1 and endogenous gene products during biosynthesis and in vitro extracellular matrix accumulation. Biochem. J. *293*(Pt 2), 387–394.

Lamande, S. R., and Bateman, J. F. (1999). Procollagen folding and assembly: the role of endoplasmic reticulum enzymes and molecular chaperones. Semin. Cell Dev. Biol. *10*, 455–464.

Lippincott-Schwartz, J., Snapp, E., and Kenworthy, A. (2001). Studying protein dynamics in living cells. Nat. Rev. Mol. Cell Biol. *2*, 444–456.

Liu, Y., Choudhury, P., Cabral, C. M., and Sifers, R. N. (1999). Oligosaccharide modification in the early secretory pathway directs the selection of a misfolded glycoprotein for degradation by the proteasome. J. Biol. Chem. *274*, 5861–5867.

Luo, H., Nakatsu, F., Furuno, A., Kato, H., Yamamoto, A., and Ohno, H. (2006). Visualization of the post-Golgi trafficking of multiphoton photoactivated transferrin receptors. Cell Struct. Funct. *31*, 63–75.

Luzio, J. P., Pryor, P. R., and Bright, N. A. (2007). Lysosomes: fusion and function. Nat. Rev. Mol. Cell Biol. *8*, 622–632.

Marini, J. C., *et al.* (2007). Consortium for osteogenesis imperfecta mutations in the helical domain of type I collagen: regions rich in lethal mutations align with collagen binding sites for integrins and proteoglycans. Hum. Mutat. *28*, 209–221.

Marutani, T., Yamamoto, A., Nagai, N., Kubota, H., and Nagata, K. (2004). Accumulation of type IV collagen in dilated ER leads to apoptosis in Hsp47-knockout mouse embryos via induction of CHOP. J. Cell Sci. *117*, 5913–5922.

Matsuoka, Y., Kubota, H., Adachi, E., Nagai, N., Marutani, T., Hosokawa, N., and Nagata, K. (2004). Insufficient folding of type IV collagen and formation of abnormal basement membrane-like structure in embryoid bodies derived from Hsp47-null embryonic stem cells. Mol. Biol. Cell *15*, 4467–4475.

Millington-Ward, S., McMahon, H. P., and Farrar, G. J. (2005). Emerging therapeutic approaches for osteogenesis imperfecta. Trends Mol. Med. *11*, 299–305.

Mizushima, N., Levine, B., Cuervo, A. M., and Klionsky, D. J. (2008). Autophagy fights disease through cellular self-digestion. Nature *451*, 1069–1075.

Mizushima, N., Yamamoto, A., Hatano, M., Kobayashi, Y., Kabeya, Y., Suzuki, K., Tokuhisa, T., Ohsumi, Y., and Yoshimori, T. (2001). Dissection of autophagosome formation using Apg5-deficient mouse embryonic stem cells. J. Cell Biol. *152*, 657–668.

Nagai, N., Hosokawa, M., Itohara, S., Adachi, E., Matsushita, T., Hosokawa, N., and Nagata, K. (2000). Embryonic lethality of molecular chaperone hsp47 knockout mice is associated with defects in collagen biosynthesis. J. Cell Biol. *150*, 1499–1506.

Nagata, K. (2003). HSP47 as a collagen-specific molecular chaperone: function and expression in normal mouse development. Semin Cell Dev. Biol. *14*, 275–282.

Oda, Y., Hosokawa, N., Wada, I., and Nagata, K. (2003). EDEM as an acceptor of terminally misfolded glycoproteins released from calnexin. Science *299*, 1394–1397.

Ogata, M., *et al.* (2006). Autophagy is activated for cell survival after endoplasmic reticulum stress. Mol. Cell Biol. *26*, 9220–9231.

Rauch, F., and Glorieux, F. H. (2004). Osteogenesis imperfecta. Lancet *363*, 1377–1385.

Ron, D., and Walter, P. (2007). Signal integration in the endoplasmic reticulum unfolded protein response. Nat. Rev. Mol. Cell Biol. *8*, 519–529.

Schnieke, A., Harbers, K., and Jaenisch, R. (1983). Embryonic lethal mutation in mice induced by retrovirus insertion into the alpha 1(I) collagen gene. Nature *304*, 315–320.

Stephens, D. J., and Pepperkok, R. (2002). Imaging of procollagen transport reveals COPI-dependent cargo sorting during ER-to-Golgi transport in mammalian cells. J. Cell Sci. *115*, 1149–1160.

Suzuki, K., and Ohsumi, Y. (2007). Molecular machinery of autophagosome formation in yeast, *Saccharomyces cerevisiae*. FEBS Lett. *581*, 2156–2161.

Ushioda, R., Hoseki, J., Araki, K., Jansen, G., Thomas, D. Y., and Nagata, K. (2008). ERdj5 is required as a disulfide reductase for degradation of misfolded proteins in the ER. Science *321*, 569–572.

Vembar, S. S., and Brodsky, J. L. (2008). One step at a time: endoplasmic reticulum-associated degradation. Nat. Rev. Mol. Cell Biol. *9*, 944–957.

Yorimitsu, T., Nair, U., Yang, Z., and Klionsky, D. J. (2006). Endoplasmic reticulum stress triggers autophagy. J. Biol. Chem. *281*, 30299–30304.

Yoshimori, T., Yamamoto, A., Moriyama, Y., Futai, M., and Tashiro, Y. (1991). Bafilomycin A1, a specific inhibitor of vacuolar-type H(+)-ATPase, inhibits acidification and protein degradation in lysosomes of cultured cells. J. Biol. Chem. *266*, 17707–17712.